

# Influence of H<sub>2</sub>SO<sub>4</sub> concentration on the performance of lead-acid battery negative plates

D. Pavlov\*, G. Petkova, T. Rogachev

*Institute of Electrochemistry and Energy Systems, Bulgarian Academy of Sciences, 1113 Sofia, Bulgaria*

Received 27 June 2007; accepted 5 September 2007

Available online 14 September 2007

## Abstract

The influence of sulfuric acid concentration on negative plate performance has been studied on 12 V/32 Ah lead-acid batteries with three negative and four positive plates per cell, i.e. the negative active material limits battery capacity. Initial capacity tests, including C20 capacity, cold cranking ability and Peukert tests, have been carried out in a wide range of sulfuric acid concentrations (from 1.18 to 1.33 sp.gr.). High initial capacity and good CCA performance were registered for batteries with acid concentration between 1.24 and 1.30 sp.gr. The charge acceptance depends on acid concentration as well as on battery state of charge. Batteries with high SoC exhibit high charge acceptance at low acid concentrations. The cycle life tests at two discharge rates (10 and 3 h discharge) evidence that sulfuric acid concentration exerts a strong effect on negative plate performance. The cycle life of batteries decreases with increase of acid concentration. The obtained results demonstrate the high impact of lead sulfate solubility on the cycle life and charge efficiency of lead-acid batteries.

© 2007 Elsevier B.V. All rights reserved.

**Keywords:** Lead-acid batteries; Lead negative plate; H<sub>2</sub>SO<sub>4</sub> electrolyte concentration; Discharge capacity; Cycle life

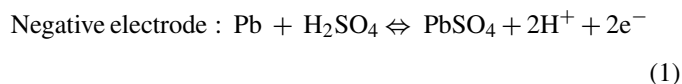
## 1. Introduction

In lead-acid batteries sulfuric acid electrolyte is an active material that participates in the cell reactions. Hence, electrolyte concentration changes on battery discharge and charge. In addition, the open-circuit voltage of a lead-acid cell is a function of electrolyte concentration according to Nernst equation. The specific resistance of the electrolyte and its freezing point, too, depend on acid concentration.

Hattori et al. [1] have established detrimental effect of higher acid concentration on the cycle life of lead-acid batteries. The effects of acid concentration and temperature on the dry-out of VRLA batteries have been studied by Bullock [2]. Several authors have tried to explain the decline in battery cycle life on the basis of linear sweep voltammetry measurements on planar lead electrode [3–5]. Yet, battery manufacturers still use high sulfuric acid concentrations in batteries for EV and HEV applications.

An earlier publication of our team [6] focused on the influence of H<sub>2</sub>SO<sub>4</sub> concentration on the performance of lead-acid battery positive plates. The aim of the present paper is to establish the influence of sulfuric acid concentration on the behavior of the negative plates.

The basic reaction on the negative electrode during discharge is formation of lead sulfate, whereby sulfuric acid is consumed. On battery charge, reduction of lead sulfate to lead proceeds and the sulfuric acid concentration increases in consistent with the charge accepted by the cell.



Several authors have studied the kinetics and mechanism of anodic oxidation of Pb to PbSO<sub>4</sub> at different electrolyte concentrations [7–10]. Kanamura and Takehara [7,8] has found that larger lead sulfate crystals form at low acid concentrations. Guo et al. [9] have reported that low acid concentration promotes the growth of large PbSO<sub>4</sub> crystals that are difficult to reduce. Das and Bose [3] have investigated the effect of sulfuric acid concentration on Pb/PbSO<sub>4</sub> electrode reactions employing linear sweep voltammetry in a wide range of concentrations. They

\* Corresponding author. Tel.: +359 2 9710083.

E-mail address: [dpavlov@labatscience.com](mailto:dpavlov@labatscience.com) (D. Pavlov).

Table 1  
Plates characteristics

Negative plates K-	
Grid PbCa	
Active material weight (g plate <sup>-1</sup> )	92
Plate thickness (mm)	1.7
Positive plates K+	
Grid PbCaSn	
Active material weight (g plate <sup>-1</sup> )	122
Plate thickness (mm)	2.1

have found that the diffusion coefficient of lead ions passes through a maximum at 5N sulfuric acid and have established that at low charging rates the kinetics of lead sulfate reduction is practically independent of acid concentration. A number of studies into the cathodic reduction of PbSO<sub>4</sub> have been reported [8–12]. Daniel and Plichon [4,5] have determined the solubility of PbSO<sub>4</sub>, the diffusion coefficient and the standard potential of Pb/Pb(II) system at different acid concentrations. They have concluded that the properties of Pb(II) are not responsible for the strong decrease in cycle life at higher acid concentration. On the contrary, many authors [8,9,11,12] consider the solubility of PbSO<sub>4</sub> crystals, which in turn depends on acid concentration, as

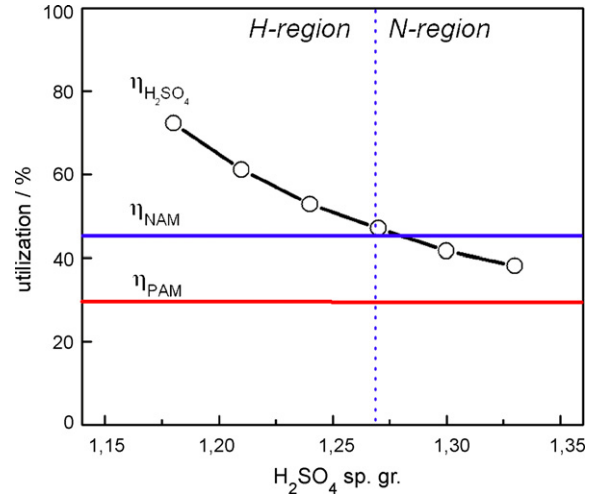


Fig. 1. Utilization of sulfuric acid, NAM and PAM as a function of H<sub>2</sub>SO<sub>4</sub> specific gravity for batteries under test.

the main factor limiting lead sulfate reduction on the negative plate.

Electrolyte concentration affects also the rate of the secondary reactions that proceed on the lead electrode like hydrogen

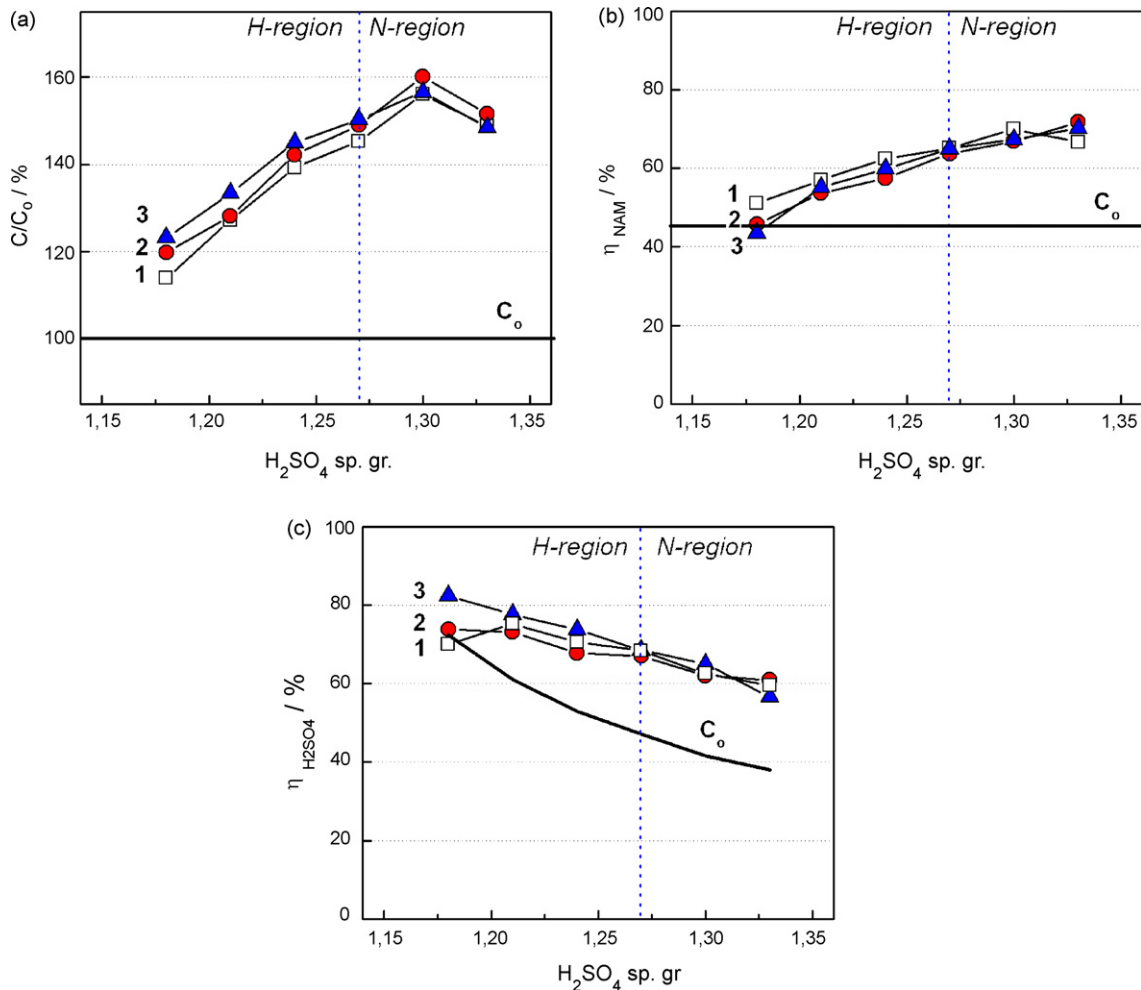


Fig. 2. Initial C<sub>20</sub> capacity test results for batteries with different H<sub>2</sub>SO<sub>4</sub> concentrations. Dependencies of: (a) capacity, (b) NAM utilization, and (c) H<sub>2</sub>SO<sub>4</sub> utilization on C<sub>H<sub>2</sub>SO<sub>4</sub></sub>.

evolution and self-discharge [3,4]. All these findings illustrate the specific and complex effect of  $H_2SO_4$  concentration on negative plate performance.

The aim of the present study is to determine the influence of sulfuric acid concentration on the performance characteristics (capacity, charge acceptance and cycle life) of batteries with capacity limited by the negative plate and to contribute to determining the optimum acid concentration in lead-acid batteries.

## 2. Experimental

### 2.1. Battery preparation

For this study standard non-formed automotive positive and negative plates produced by battery plant “START” in the town of Dobrich, Bulgaria, were used. The main characteristics of the plates are presented in Table 1.

Tank formation of the plates was carried out in 1.06 sp.gr.  $H_2SO_4$  for 18 h, employing a multi-step algorithm developed in our laboratory, until 220% of the theoretical capacity was reached.

After formation the plates were assembled into 12 V/32 Ah batteries comprising three negative and four positive plates per cell. Thus, the negative active material limited battery capacity and hence the effect of sulfuric acid concentration on negative plate performance would be pronounced more clearly. AGM separator (H&V, USA) with a thickness of 3 mm ( $425 \text{ g m}^{-2}$ ) was used under 20% compression. The cells were filled with 530 ml of electrolyte per cell. The following  $H_2SO_4$  concentrations were used in this investigation: 1.18, 1.21, 1.24, 1.27, 1.30 and 1.33 sp.gr.

The rated capacity,  $C_o=32 \text{ Ah}$ , was calculated at 45% utilization of the negative active material at 20 h discharge rate and the corresponding utilization of PAM was calculated as 29.3%.

### 2.2. Initial capacity tests

All battery tests were carried out using Bitrode testing equipment.

First, the batteries were subjected to initial  $C_{20}$  capacity test, cold cranking ability test and Peukert dependence determination. In these tests battery charge was conducted in three steps: first step  $I_{ch}=24.5 \text{ A}$  with voltage limit 14.8 V; second step

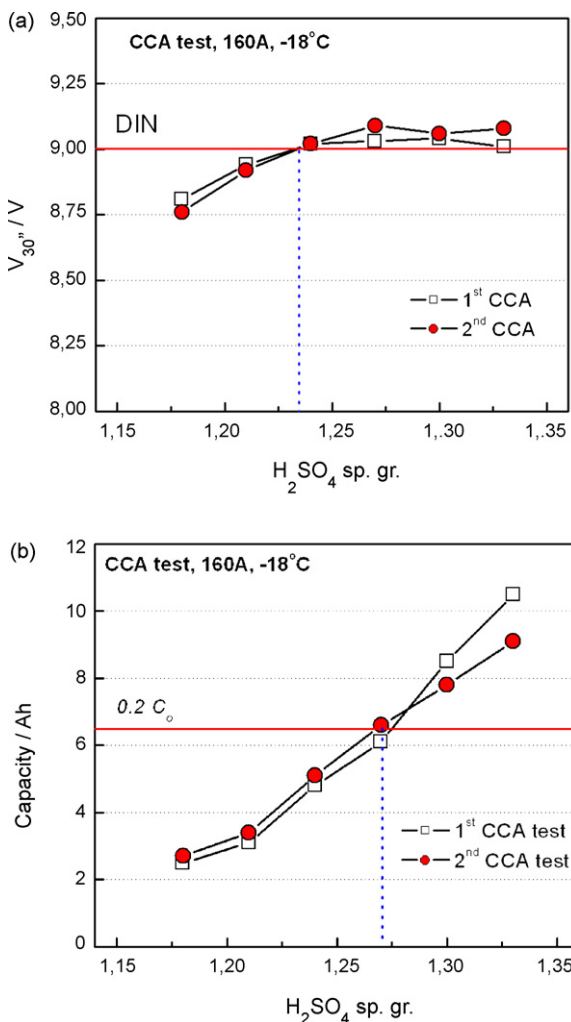


Fig. 3. Initial CCA performance for batteries with different  $H_2SO_4$  concentrations. (a)  $V_{30r}$  and (b) CCA capacity dependences on  $CH_2SO_4$ .

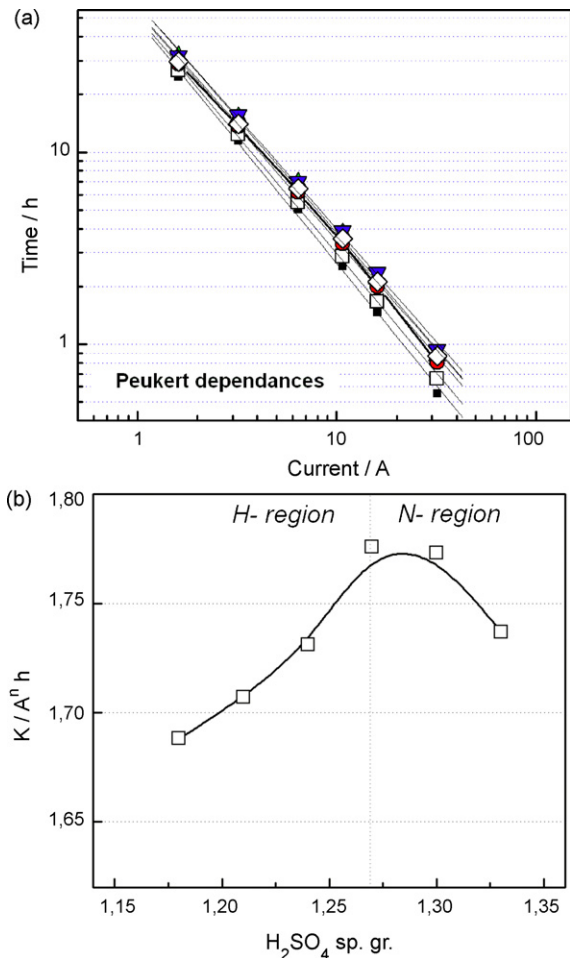


Fig. 4. (a) Peukert dependences for tested batteries. (b) Constant  $K$  in Peukert equations as a function of acid concentration.

$U = 14.8$  V up to 110% overcharge, and third step  $I_{ch} = 2$  A to 115% overcharge.

2.3. Battery cycling tests

The batteries were cycled at two different discharge rates:  $C_{10}$ , 10 h discharge rate ( $I_{disch} = 3.2$  A) and  $C_3$ , 3 h discharge rate ( $I_{disch} = 10.5$  A). Discharge was conducted down to 10.70 V (at  $C_{10}$ ) and 9.60 V (at  $C_3$ ), respectively. Battery charge was performed with  $I = 16$  A with voltage limit of 15 V and then at 15 V to 110% overcharge. During the third step the charge continued with  $I = 2$  A to 115% overcharge. The rest period after charge was 30 min. All cycle life tests were conducted at 25 °C. The end of battery life was set at 80% of the rated capacity for  $C_{10}$  discharge and 70% at  $C_3$  cycling, respectively.

On completion of the cycle life tests the negative active materials were set to various analyses as follows: chemical analysis, X-ray diffraction analysis, SEM observations, BET surface measurements and porometric measurements.

3. Results and discussion

3.1. Utilization of the active materials

Fig. 1 presents the utilization of sulfuric acid ( $\eta_{H_2SO_4}$ ) for the tested batteries as a function of  $H_2SO_4$  specific gravity. The utilization coefficients of NAM and PAM for 20 h discharge rate are also shown in the figure.

Two regions can be distinguished with regard to the utilization of  $H_2SO_4$ :

- (i)  $C_{H_2SO_4} < 1.27$  sp.gr.: The utilization coefficient of  $H_2SO_4$  is higher than those of NAM and PAM, and hence sulfuric acid limits battery capacity in this region of concentrations. Therefore, let us name this region of concentration “H-region”.
- (ii)  $C_{H_2SO_4} > 1.27$  sp.gr.: The utilization coefficient of NAM is the highest and hence the negative plates will limit the capacity. Let us call this  $H_2SO_4$  concentration region “N-region”.

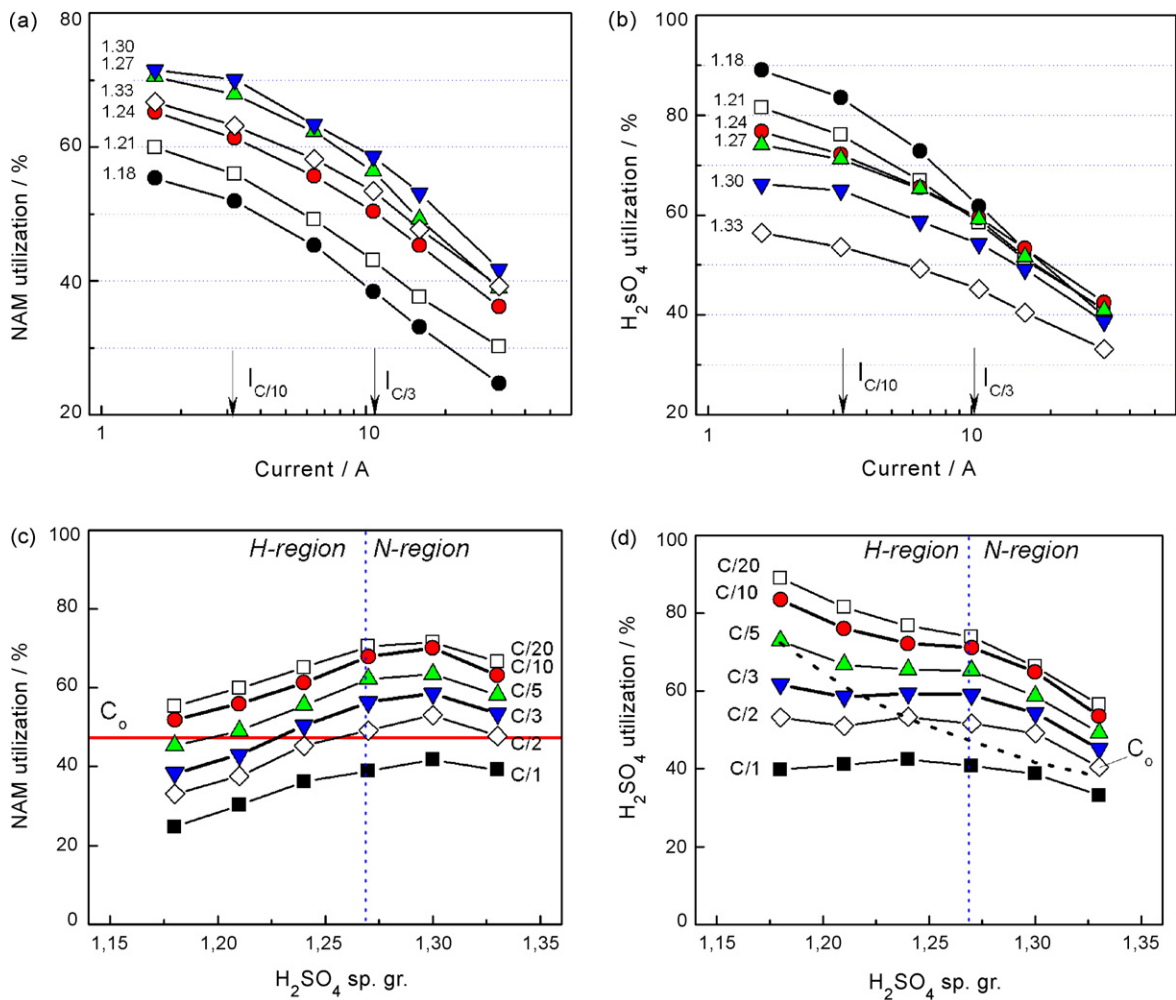


Fig. 5. Dependences calculated from Peukert measurements: (a) NAM utilization and (b) sulfuric acid utilization vs. discharge current; (c) NAM utilization and (d) sulfuric acid utilization vs.  $C_{H_2SO_4}$ .

Table 2  
Peukert dependences at different acid concentrations

H <sub>2</sub> SO <sub>4</sub> sp.gr.	1.18	1.21	1.24	1.27	1.30	1.33
Peukert	$I^{1.26}t = 1.68$	$I^{1.23}t = 1.70$	$I^{1.19}t = 1.73$	$I^{1.19}t = 1.77$	$I^{1.17}t = 1.77$	$I^{1.18}t = 1.73$

The influence of H<sub>2</sub>SO<sub>4</sub> concentration on battery capacity, cold cranking performance, cycle life and charge acceptance will be discussed for the two concentration regions.

### 3.2. Initial capacity tests

Initial performance tests included three C<sub>20</sub> capacity measurements at 25 °C, and two cold cranking ability (CCA) tests at –18 °C. Fig. 2 presents the obtained three initial C<sub>20</sub> capacities of the batteries, as well as the utilization of NAM and sulfuric acid as a function of H<sub>2</sub>SO<sub>4</sub> concentration. All batteries meet the standard requirement to deliver 100% of the rated capacity during the initial cycles. With increase of acid concentration the C<sub>20</sub> capacity of the batteries increases. The C<sub>20</sub> values pass through a maximum at 1.30 sp.gr. and decrease at H<sub>2</sub>SO<sub>4</sub> concentration of 1.33 sp.gr. For lower acid concentrations the values of the second and third capacity measurements are higher compared to the first one. For 1.30 and 1.33 sp.gr. the capacity during the third cycle declines slightly relative to that during the second cycle.

Fig. 2b and c shows that with increase of H<sub>2</sub>SO<sub>4</sub> concentration the utilization of NAM increases, while the H<sub>2</sub>SO<sub>4</sub> utilization decreases. In the H-region of acid concentrations (C<sub>H<sub>2</sub>SO<sub>4</sub></sub> < 1.27 sp.gr.) the utilization of NAM varies between 40 and 63%, while that of H<sub>2</sub>SO<sub>4</sub> is between 68 and 80%. During these capacity tests the discharge current ( $I_{\text{disch}} = C_0/20$  A) is fairly low and H<sub>2</sub>SO<sub>4</sub> has sufficient time to diffuse from the bulk electrolyte to the inner parts of the plates. The whole electrolyte volume in the lead-acid cell is involved in the current generation processes and hence the utilization of H<sub>2</sub>SO<sub>4</sub> is high.

In the N-region (C<sub>H<sub>2</sub>SO<sub>4</sub></sub> > 1.27 sp.gr.) the utilization of H<sub>2</sub>SO<sub>4</sub> is from 57 to 68%, while the NAM utilization is between 63 and 70%. These values of  $\eta_{\text{NAM}}$  are rather high and the negative plates determine the capacity of the batteries. At 1.33 sp.gr. H<sub>2</sub>SO<sub>4</sub>, 70% utilization of NAM is fairly high and the capacity is lower as compared to that at 1.30 sp.gr. H<sub>2</sub>SO<sub>4</sub> ( $\eta_{\text{NAM}} = 67\%$ ) (Fig. 2a). Most probably, this is a result of passivation phenomena on the negative plates.

### 3.3. Cold cranking ability tests

Two CCA discharge tests were conducted according to the DIN43539-2 test standard protocol with  $I = 5C_{20}$  at –18 °C. The dependences of battery voltage at the 30th second of discharge ( $V_{30''}$ ) and CCA capacity on acid concentration are presented in Fig. 3a and b, respectively. It is evident from Fig. 3a that  $V_{30''}$  increases with increase of acid concentration up to 1.24 sp.gr. At electrolyte concentrations higher than 1.24 sp.gr.,  $V_{30''}$  does not change with further increase in acid concentration. The obtained results may be due to increase in specific electroresistivity in dilute sulfuric acid solutions at low temperatures [13].

Fig. 3b indicates that the CCA capacity increases almost linearly with increase of acid concentration with a slope of 0.48 Ah per 0.01 sp.gr. of H<sub>2</sub>SO<sub>4</sub>. It should be noted that the batteries with acid concentration above 1.24 sp.gr. meet the requirements of the DIN standard, namely 9.0 V at 30th second of discharge and cold cranking capacity of 0.2C<sub>20</sub>. Under the CCA discharge conditions the utilization of all active materials (PAM, NAM and H<sub>2</sub>SO<sub>4</sub>) is less than 10.5% in the entire range of H<sub>2</sub>SO<sub>4</sub> concentrations.

### 3.4. Peukert dependences

To establish the effect of acid concentration on the discharge performance at different current densities, Peukert dependences were measured at C/20, C/10, C/5, C/3, C/2 and C/1 rates. Fig. 4a shows that all batteries follow the Peukert equation  $I^n t = K$ . The

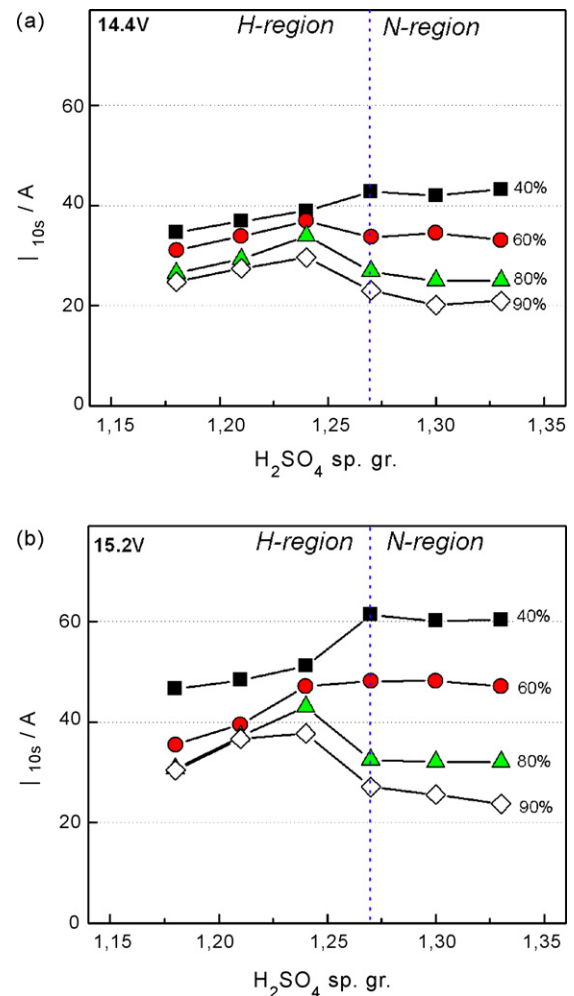


Fig. 6. Charge acceptance ( $I_{10s}$ ) at different SoC: (a) 14.4 V and (b) 15.2 V voltage limits.

calculated  $n$  and  $K$  values are presented in Table 2. The  $n$  coefficients decrease with increase of acid concentration. Fig. 4b presents the  $K$  constant as a function of acid concentration. It can be seen that the values of  $K$  increase in the H-region of acid concentrations and reach a maximum at 1.27 sp.gr. In the N-region,  $K$  decreases at  $C_{H_2SO_4} = 1.33$  sp.gr. The physical meaning of  $K$  is available capacity and this explains the similar trend of the dependences of  $K$  (Fig. 4b) and  $C_{20}$  capacity (Fig. 2a) on  $H_2SO_4$  concentration.

The utilization coefficients of NAM and  $H_2SO_4$  were calculated based on the experimental Peukert dependences. Fig. 5 presents the dependences of  $\eta_{NAM}$  and  $\eta_{H_2SO_4}$  on discharge current and on sulfuric acid concentration. Fig. 5a and b evidence that with increase of discharge current, the utilization of NAM and  $H_2SO_4$  decreases. The dependences of NAM and  $H_2SO_4$  utilization on sulfuric acid concentration are presented in Fig. 5c and d. The utilization of NAM increases with increase of  $C_{H_2SO_4}$ , reaches a maximum at  $C_{H_2SO_4} = 1.30$  sp.gr. and decreases at  $C_{H_2SO_4} = 1.33$  sp.gr. The  $H_2SO_4$  utilization at low discharge currents ( $I = C/10$  and  $I = C/20$  A) decreases with increase of  $C_{H_2SO_4}$ . In the H-region of acid concentrations, the  $\eta_{H_2SO_4}/C_{H_2SO_4}$  relationships are almost independent of  $H_2SO_4$

concentration at discharge currents between  $C/5$  and  $C/2$ . In the N-region,  $\eta_{H_2SO_4}$  decreases slightly with increase of  $C_{H_2SO_4}$ . At discharge current  $I = C/1$  A, the  $H_2SO_4$  utilization is almost equal within the entire range of electrolyte concentrations.

### 3.5. Charge acceptance tests

The charge acceptance of the batteries at different states of charge (SoC) was determined from the current at the 10th second of charge ( $I_{10s}$ ) for two voltage limits, 14.4 and 15.2 V. The obtained results are presented in Fig. 6. The two characteristic concentration regions, H-region and N-region, are clearly distinguished for both charge voltages. In the H-region, the charge acceptance ( $I_{10s}$ ) depends but slightly on SoC for both charge voltages, while in the N-region the state of charge influences strongly the charge acceptance. Within the investigated concentration range the values of  $I_{10s}$  at 15.2 V are considerably higher than those obtained at 14.4 V. This may be related to gassing reactions that proceed readily at higher voltages.

The data in Fig. 6 evidence that high charge acceptance is achieved at lower state of charge for both charge voltages in the entire  $H_2SO_4$  concentration range. At SoC = 40% the highest

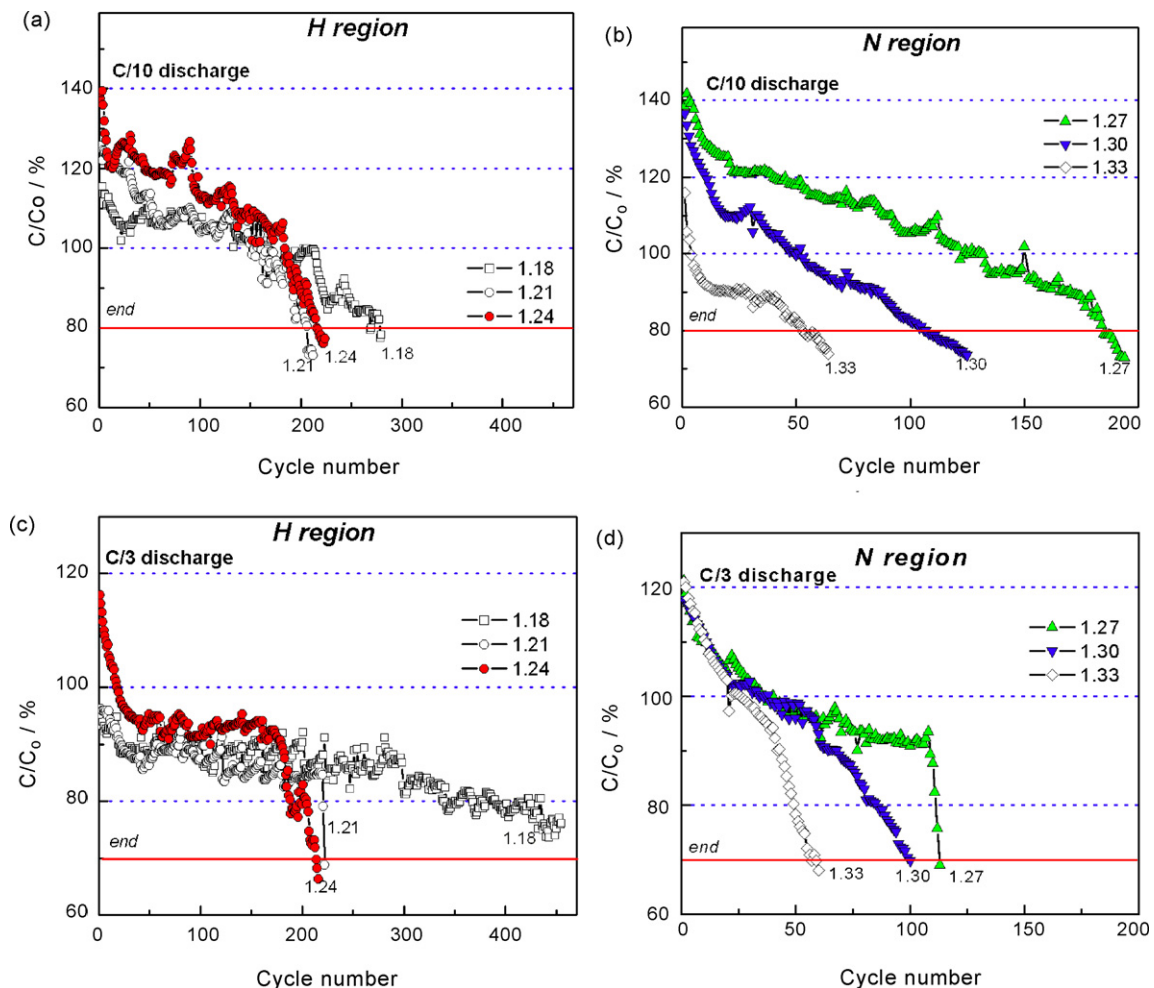


Fig. 7. Cycle life test results for batteries with different acid concentrations: (a and c) H-region; (b and d) N-region; at different discharge rates: (a and b)  $I = C/10$  A; (c and d)  $I = C/3$  A.

charge acceptance is obtained within the N-region. At SoC = 80 and 90% the charge acceptance in the H-region is higher than in the N-region of acid concentrations. Hence, batteries operating at higher state of charge should be filled with electrolyte with concentration lower than 1.27 sp.gr.

### 3.6. Cycle life tests

Batteries with different sulfuric acid concentrations were set to cycle life tests at  $C/10$  and  $C/3$  discharge rates. Fig. 7 presents the obtained capacity vs. cycle number curves for the H- and N-concentration regions. Battery cycle life performance depends strongly on  $H_2SO_4$  concentration.

Two periods can be distinguished in the capacity/cycle number curves:

#### 3.6.1. Initial period

During this period the capacity of the batteries declines quickly to a certain value. The NAM and PAM structures obtained during the formation process are transformed into operative structures. The spongy lead structure of NAM is produced by electrochemical reduction of PbO and 3BS ( $3PbO \cdot PbSO_4 \cdot H_2O$ ) in diluted sulfuric acid solution at  $C_{H_2SO_4} = 1.06$  sp.gr.). The data in Fig. 7 evidence that this structure of NAM provides high initial capacity. During battery operation lead sulfate is formed on discharge, which is then reduced back to lead on charge and thus the initially formed NAM structure is partially destroyed.

The charge/discharge processes proceed under quite different conditions, in terms of reaction precursor and electrolyte concentration, compared to the process of formation. This leads to transformation of the NAM structure and, as can be seen from Fig. 7, to capacity decline.

#### 3.6.2. Second period

During this period the capacity of the batteries decreases slightly and after a certain time of cycling starts to decline. The reversibility of the processes that occur in the operating NAM structure determines the capacity decrease on cycling and the cycle life of the batteries. Fig. 7 indicates that electrolyte concentration exerts a strong influence on these processes during cycling. The cycling behavior of the batteries differs significantly for the two  $H_2SO_4$  concentration regions.

It is evident that in the N-region of concentrations, where NAM limits battery capacity, the cycle life is shorter than that in the H-region. Batteries with  $C_{H_2SO_4} = 1.33$  sp.gr. have a cycle life of 50 cycles for both discharge currents (Fig. 7b and d). The cycle life of the battery with  $C_{H_2SO_4} = 1.27$  sp.gr. increases to 180 cycles for  $C/10$  discharge rate (Fig. 7b). Fig. 7d shows that the battery with this latter concentration endures 110 cycles at  $C/3$  discharge rate. Most probably, some unidentified irreversible process shortens the life of the battery, so actually the influence of sulfuric acid concentration remains uncertain.

In the H-region of acid concentrations the amount of  $H_2SO_4$  limits battery capacity. The life of the batteries is longer than 200 cycles for both discharge current densities. At  $C_{H_2SO_4} = 1.18$  sp.gr., the cycle life reaches 400 cycles for  $I = C/3$  A. The

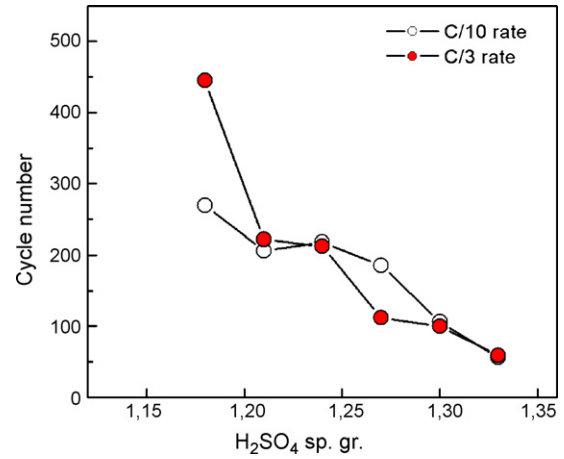


Fig. 8. Battery cycle life as a function of  $H_2SO_4$  concentration.

longer cycle life of batteries with electrolyte concentrations within the H-region is probably due to relatively low degree of NAM utilization (Fig. 5c) and the more effective processes of charge and discharge. Based on data in Fig. 7 we assume that in the H-region of acid concentrations the processes that contribute to building the operating NAM structure proceed with a

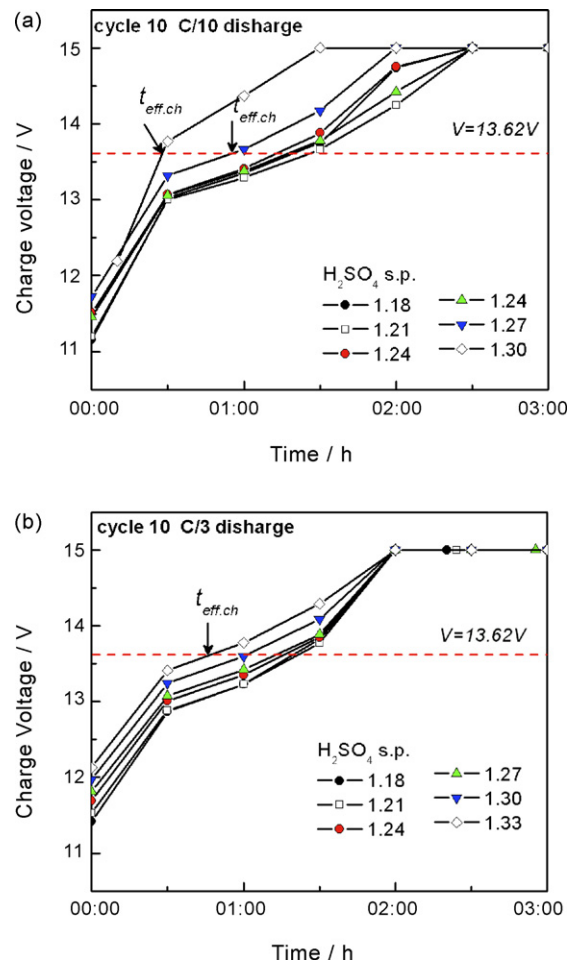


Fig. 9. Battery charge voltage vs. time of charge at 10th cycle: (a)  $C/10$ , and (b)  $C/3$  discharge rate.

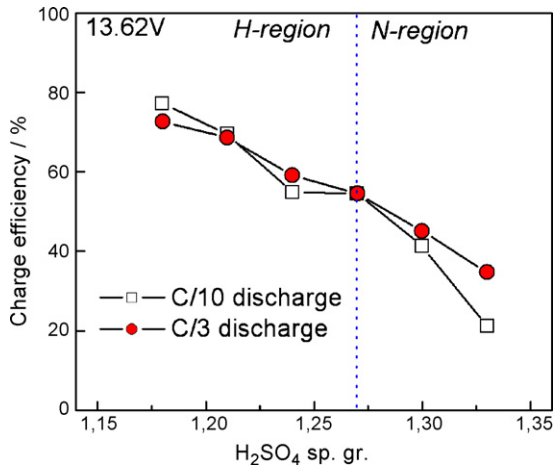


Fig. 10. Battery charge efficiency as a function of H<sub>2</sub>SO<sub>4</sub> concentration.

high degree of reversibility. On charge, the operating structure of NAM is recovered completely thus ensuring longer battery cycle life. The cycle life of batteries with electrolyte concentrations within the H-region is also limited by side effects (Fig. 7c, C<sub>H2SO4</sub> = 1.21 sp.gr.) and probably corrosion of the positive grid, too, has such effect.

The data in Fig. 7a and c evidence that discharge current strongly influences battery capacity on cycling. At I = C/10 A, the capacity decreases slowly from 120 to 90% and then a rapid capacity decline follows. At I = C/3 A, the capacity is arrested between 95 and 85% and thus the battery operates with lower discharge capacity.

Fig. 8 presents the cycle life results for the batteries under test as a function of H<sub>2</sub>SO<sub>4</sub> concentration for both discharge currents. It can be seen that the cycle life decreases with increase of C<sub>H2SO4</sub> in the entire concentration range.

### 3.7. Charge efficiency

The effect of acid concentration on battery charge behavior during cycling was studied for both discharge rates. Fig. 9

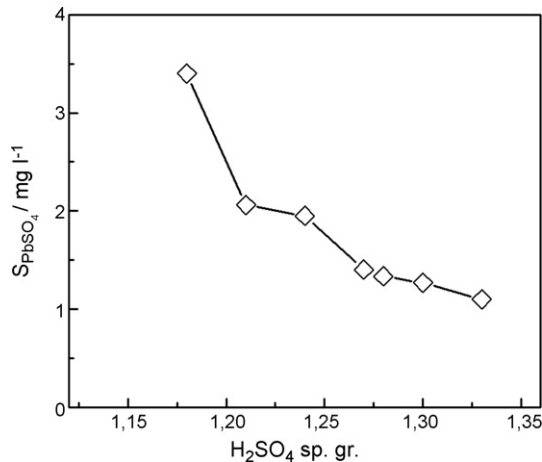


Fig. 11. Dependence of the solubility of PbSO<sub>4</sub> crystals on H<sub>2</sub>SO<sub>4</sub> concentration, as determined by Daniel and Plichon [4].

presents the voltage/time charge curves for batteries with different H<sub>2</sub>SO<sub>4</sub> concentrations after the 10th discharge. The profiles of the obtained charge curves indicate that the charge process depends on H<sub>2</sub>SO<sub>4</sub> concentration and on discharge current. The value of 13.62 V (2.27 V cell<sup>-1</sup>) was accepted as upper voltage limit for effective charge, above which water decomposition

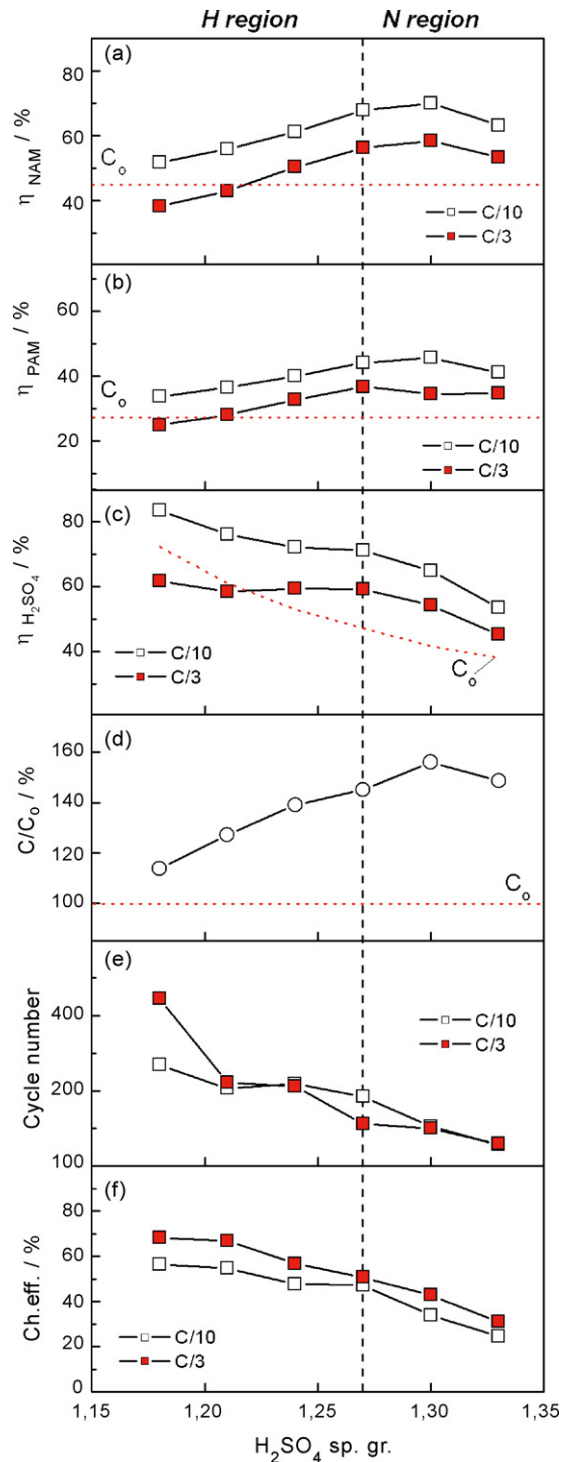


Fig. 12. Dependences of: (a) NAM utilization; (b) PAM utilization; (c) H<sub>2</sub>SO<sub>4</sub> utilization; (d) initial C<sub>20</sub> capacity; (e) cycle life, and (f) charge efficiency on acid concentration.



starts. The time to achieve this voltage limit ( $t_{\text{eff.ch}}$ ) and the corresponding charge capacity can be used as a measure of charge efficiency. Charge efficiency (Ch.eff.) can be determined by the following relation:

$$\text{Ch.eff.} = \frac{I_{\text{ch}} t_{\text{eff.ch}}}{C_{n-1}}$$

$I_{\text{ch}} t_{\text{eff.ch}}$  is the quantity of electricity passed through the battery for  $t_{\text{eff.ch}}$  period,  $C_{n-1}$  is the capacity during the preceding discharge cycle. This parameter differs from the charge acceptance discussed in the previous section. While charge acceptance determines the power of the battery on charge, charge efficiency characterizes the quantity of electrical charge return in the battery before the beginning of water decomposition versus battery capacity during the preceding discharge. Fig. 10 presents the dependences of charge efficiency on sulfuric acid concentration for the batteries under test. Batteries with electrolyte concentrations within the H-region exhibit higher charge efficiency, which decreases slightly with increase of  $C_{\text{H}_2\text{SO}_4}$ . In the N-region of acid concentrations, the charge efficiency decreases substantially with increase of acid concentration for both discharge rates. An increase of acid concentration above 1.27 sp.gr. impedes battery charge.

### 3.8. Dependence of $\text{PbSO}_4$ solubility on sulfuric acid concentration

Irreversible formation of lead sulfate is one of the main reasons for capacity decay of lead negative plates. It is known [11,12] that solubility of  $\text{PbSO}_4$  limits lead sulfate reduction and thus the charge process of the negative plate becomes ineffective. On the other hand, solubility of lead sulfate depends on  $C_{\text{H}_2\text{SO}_4}$  [4,14–15] and, therefore, the question of the relation between  $\text{PbSO}_4$  solubility and acid concentration at negative plate is very important. Fig. 11 presents the dependence of lead sulfate solubility on acid concentration, based on data provided by Daniel and Plichon [4]. When comparing the data in Figs. 8 and 11, it is obvious that the two curves have similar profile. This suggests that  $\text{PbSO}_4$  solubility is the factor with high impact on battery cycle life. It is evident from the data in Figs. 10 and 11 that both charge efficiency and  $\text{PbSO}_4$  solubility decrease with increase of  $C_{\text{H}_2\text{SO}_4}$ . It can be concluded that, the increased charge efficiency is due to the increased solubility of  $\text{PbSO}_4$  at low  $\text{H}_2\text{SO}_4$  concentrations.

## 4. Conclusions

The results of the present work indicate that by changing sulfuric acid concentration, at constant volume of electrolyte and

constant amount of NAM and PAM, two regions of different battery behaviors can be distinguished, depending on  $C_{\text{H}_2\text{SO}_4}$ : H-region, in which sulfuric acid limits battery performance, and N-region, in which NAM limits the behavior of the batteries. Fig. 12 compares the dependences of active material utilization and battery parameters on sulfuric acid concentration in the batteries.

In the H-region of acid concentrations, the utilization of NAM and PAM decreases, while that of  $\text{H}_2\text{SO}_4$  increases with decrease of acid concentration from 1.27 to 1.18 sp.gr. Batteries with electrolytes within this region of acid concentrations have lower initial capacity ( $C_0$ ), longer cycle life and higher charge efficiency.

In the N-region of acid concentrations, the utilization of NAM and PAM increases with increase of acid concentration reaching a maximum at 1.30 sp.gr. and then decreases slightly at 1.33 sp.gr. The utilization of  $\text{H}_2\text{SO}_4$  declines substantially. This results in higher initial capacity, shorter cycle life and reduced charge efficiency of the batteries.

This study demonstrates that the specific influence of  $C_{\text{H}_2\text{SO}_4}$  on battery performance depends on the type of capacity limiting active material in the battery. As the amounts of the different active materials (lead, lead dioxide and  $\text{H}_2\text{SO}_4$ ) in a lead-acid battery are primarily determined during the battery design process, it is possible to define different battery behaviors.

The results of this investigation provide additional information on the parameters that should be considered for appropriate selection of electrolyte concentration in view of the specific application and service requirements for a lead-acid battery.

## References

- [1] S. Hattori, S. Tosano, O. Kusuoka, *Denki Kagaku* 44 (1976) 792.
- [2] K. Bullock, *J. Power Sources* 116 (2003) 8–13.
- [3] K. Das, K. Bose, *Bull. Electrochem.* 2 (1986) 387.
- [4] V. Daniel, V. Plichon, *Electrochim. Acta* 27 (1982) 771–774.
- [5] V. Daniel, V. Plichon, *Electrochim. Acta* 28 (1983) 781–784.
- [6] D. Pavlov, V. Naidenov, S. Ruevski, *J. Power Sources* 161 (2006) 658–665.
- [7] K. Kanamura, Z. Takehara, *J. Electrochem. Soc.* 139 (1992) 345–351.
- [8] Z. Takehara, *J. Power Sources* 85 (2000) 29.
- [9] Y. Guo, L. Niu, S. Zhang, S. Chen, *J. Power Sources* 85 (2000) 38.
- [10] D. Simonsson, P. Ekdunge, M. Lindgren, *J. Electrochem. Soc.* 135 (1988) 1613.
- [11] G. Petkova, D. Pavlov, *J. Power Sources* 113 (2003) 355–362.
- [12] M. Thele, E. Karden, E. Surewaard, D.U. Sauer, *J. Power Sources* 158 (2006) 953–963.
- [13] L. Prout, *J. Power Sources* 51 (1994) 463–487.
- [14] G.W. Vinal, D.N. Craig, *J. Res. Natnl. Bur. Stand.* 10 (1933) 781.
- [15] G.W. Vinal, D.N. Craig, *J. Res. Natnl. Bur. Stand.* 14 (1935) 449.